University of Science and Technology of Hanoi

Mean-field study of the equation of states of nuclear matter and tidal deformation of neutron star

Bachelor Thesis

Author:
Nguyen Hoang Dang Khoa

Supervisors:
Prof. Dao Tien Khoa
Dr. Ngo Hai Tan

June 26, 2021

Contents

List of Abbreviations

BH	Black hole
BHF	Brueckner-Hartree-Fock
CFL	Confident level
DU	Direct Urca
EoS	Equation of States
GE	Gravito-electric
GM	Gravito-magnetic
GR	General Relativity
GRB	Gamma-ray burst
GW	Gravitational wave
HF	Hartree-Fock
NM	Nuclear Matter
NN	Nucleon-Nucleon
NS	Neutron Star
PSR	Pulsar
TOV	Tolmann-Oppenheimer-Volkoff

List of Tables

List of Figures

Chapter 1

Introduction

Neutron stars (NS) are star-like astronomical objects with mass M on the order of solar mass ($M_\odot$), a radius of $\sim 10 - 12\ km$ and an average density n several times greater than that of nucleon ($n_0 \approx 0.17\ fm^{-3}$). They are arguably the densest accessible objects, excluding black holes which we know nothing about inside the event horizon, in the universe (Baym and Pethick, 1975). Due to extremely high density, the matter on NS mainly consists of neutrons that are closely packed together with a small percentage of other particles (p, e^-, ...), similar to a atomic nucleus on macroscopic scale. For this reason, they are also the ideal objects for testing physical theories of dense matter and provide connections between different field of physics, i.e. nuclear physics, elementary particle physics and astrophysics (Lattimer and Prakash, 2004).

During the NS's formation process, protons (p) and electrons (e^-) combined together to form neutrons, i.e.

$$p + e^- \longrightarrow n + \nu_e \tag{1.1}$$

and the star only holds itself against gravity by its own degeneracy pressure and strong force repulsion, which explains why the matter on NS is neutron-dominant and hence the name "neutron stars". After the NS is formed, energy quickly dissipates through neutrino emission, resulting in a relatively cold NS. In this study, we will only concern with the NS after a considerable time from its formation, when the temperature is considered to be $T = 0\ K$.

On a NS, the matter exists as an inhomogenous, low-density *crust* and gradually becomes a more uniform *core* the closer to the NS center as in Figure 1.1. In order to study about the properties of NS matter, the problem have to be approached from the nuclear physics point of view, where we study about *nuclear matter* (NM). For a nuclear system as massive as a NS, we consider one with infinite number of nucleons that are in β-stable state with a small portion of leptons, in which the properties of matter are described using an *equation of states* (EoS), i.e. the relation between different state variables (pressure P, mass-energy density ε, ...) of the system. Ideally, the EoS can be derived from the interactions of quarks under strong force in the framework of quantum chromodynamics. However, due to this having yet to be possible at the moment, the EoS of NM is instead interpreted from a nonrelativistic mean-field study approach with several updated versions of the realistic density-dependent CDM3Yn interaction models (Khoa et al., 1995; Khoa and Cuong, 2007) using Hartree-Fock (HF) formalism, which will be implemented further in Chapter 2.

Following the gravitational wave (GW) signals GW170817 (Abbott et al., 2017) and GW190425

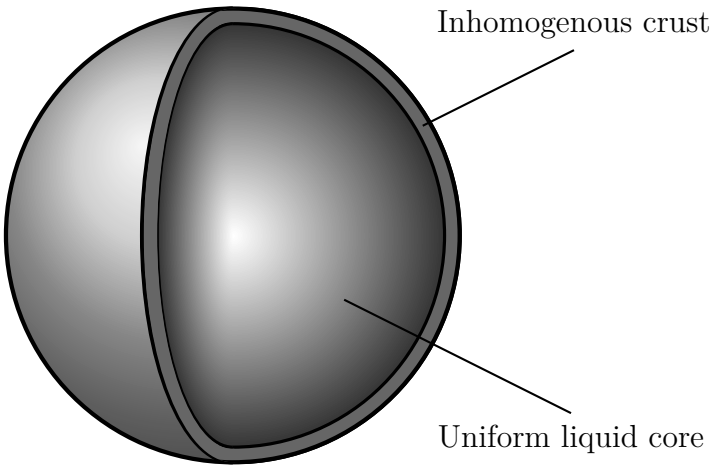

Figure 1.1: Neutron star's overall structure. The baryon density decreases (from white to dark gray) as we move outward from the NS center.

(Abbott et al., 2020) from two binary NS mergers observed by LIGO and Virgo laser interferometer in 17$^{\text{th}}$ August 2017 and 25$^{\text{th}}$ April 2019 respectively, the tidal deformation of the NS can be further constrained, as well as the mass M and radius R of the NS (Abbott et al., 2018). The NS merger event is illustrated as in Figure 1.2.

Apparently, the EoS of high-density NM plays the most important role in deciding the macroscopic properties of NS. In particular, given the EoS of the crust from the compressible liquid drop model and by using the EoS of the uniform NS core from the result of the HF calculation of cold β-stable NM, the gravitational mass and radius of the star can be decided by the framework of General Relativity (GR) (Tan et al., 2020, 2021), i.e. the Tolman-Oppenheimer-Volkoff (TOV) equation, which will in turn be compared to the observational astrophysical constraints to deduce the most suitable EoS of the constituent NS in this system.

In addition, due to the enormous mass, each NS possesses powerful gravitational field and therefore, they tend to "stretch out" their companion under the tidal effect as in Figure 1.2, while orbiting spirally toward each others and dissipating energy under the form of GW. Particularly, the shape and mass-energy distribution of the NS are tidally deformed from its supposedly spherical shape, resulting in nonzero multipole moments (Hinderer, 2008; Hinderer et al., 2010; Damour and Nagar, 2009). The NS's reaction, i.e. how strongly it deforms when being under a tidal field, is expressed in terms of the *tidal Love numbers* k_l of several orders l, where in this study, we will evaluate the Love number of NS up to the 4$^{\text{th}}$ order, i.e. $l = 2, 3, 4$ (Perot and Chamel, 2021). Apparently, the tidal Love number depends heavily on the EoS of matter and this dependence will be further emphasized in Chapter 3. For NS, the central density can be up to $6n_0$ and possesses a Love number of order ~ 0.1, while our Earth has that of 0.3. In a recent study, the Love number was calculated for spinning black holes, which showed that even with nearly infinite density, they still posess a small Love number of 0.002 (Le Tiec and Casals,

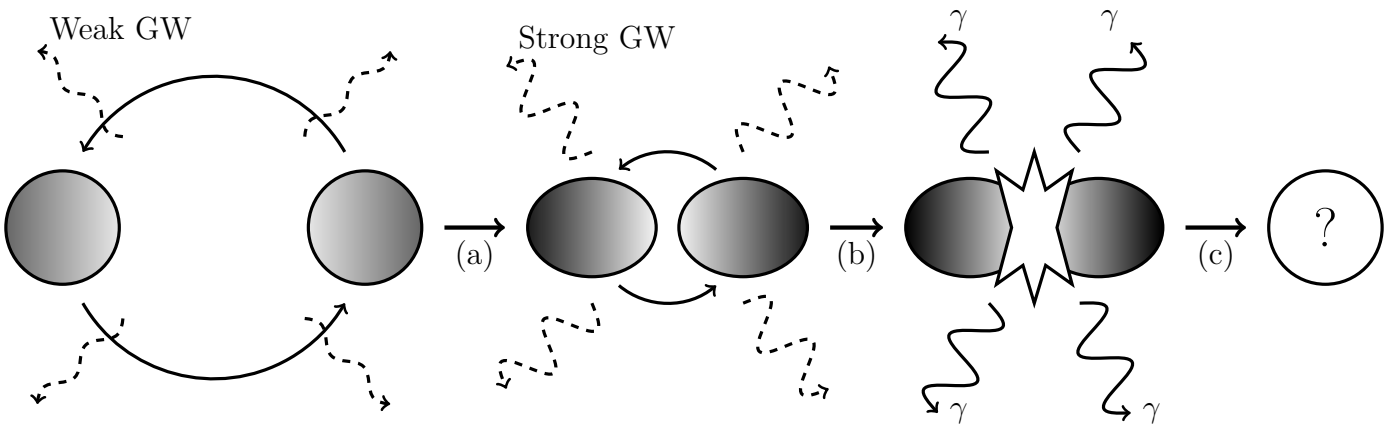

Figure 1.2: Illustration of binary NS merger. (a) The two companion NSs orbit about each others, while gradually losing energy through weak GW and come closer with time. (b) As the two NS get closer, they accelerate and emit stronger GW until (c) colliding, which results in a *kilonova*, characterized by a short *gamma ray burst* (GRB). The product of the merger has yet been decided to be a black hole (BH) or another NS.

2021).

Furthermore, under small perturbation of spacetime, the tidal field can also be separated into two components: the *gravito-electric* (GE) and *gravito-magnetic* (GM) terms (Damour and Nagar, 2009) that are analogous to that in eletromagnetic field. As a result, the deformation of the NS, i.e. Love numbers, in the perturbed tidal field can also be categorized into the corresponding GE (k_l) and GM (j_l) components (Perot and Chamel, 2021), whose result will be presented in more details in Chapter 3. To sum up, this study is dedicated to:

- Include the spin polarization effect to the existing CDM3Yn models (Tan et al., 2021),
- Assess the dependence of NS's gravitational mass and radius to different EoS,
- Investigate the sensitivity of GE and GM tidal deformability and Love numbers to NM properties,
- Compare some of the NS's calculated properties to the astrophysical constraints obtained experimentally.

Chapter 2

Hartree-Fock Formalism of Nuclear Matter

2.1 Nucleon-Nucleon Interaction

Due to the lack of a exact theory to describe the nucleon-nucleon (NN) interaction, a model need to be imposed and fit with experimental measurement or theoretical calculation results. Plus, for a system as massive as a NS, deducing the EoS using the *ab initio* method, i.e. solving the Schrödinger equation over all particles, is simply impossible, therefore an *effective interaction* must be used (Greiner and Maruhn, 1996). In this section, we only limit ourselves to two-body interaction, thus, the NN potential can be expressed in the form of

$$v = v(\boldsymbol{r}, \boldsymbol{r'}, \boldsymbol{p}, \boldsymbol{p'}, \boldsymbol{\sigma}, \boldsymbol{\sigma'}, \boldsymbol{\tau}, \boldsymbol{\tau'}) \tag{2.1}$$

where the primed and unprimed variables indicate the properties of 2 nucleons respectively, in which $\boldsymbol{r}$ is the particle's position, $\boldsymbol{p}$ is its momentum, $\boldsymbol{\sigma}$ is its intrinsic spin and $\boldsymbol{\tau}$ is its isospin.

The functional form of v in (2.1) cannot freely take any form but is constrained by many invariance requirements (Greiner and Maruhn, 1996), namely the translational, Galilei, rotational, isospin, parity and time reversal invariance. Having such considerations, developing further the M3Y-Paris interaction, which was used by the HF study of NM (Loan et al., 2011; Tan et al., 2016, 2020, 2021) and the folding model study of NN scattering (Khoa et al., 1997; Khoa and Satchler, 2000),

$$v = v_{00}(r) + v_{10}(r)\boldsymbol{\sigma}\cdot\boldsymbol{\sigma'} + v_{01}(r)\boldsymbol{\tau}\cdot\boldsymbol{\tau'} + v_{11}(r)(\boldsymbol{\sigma}\cdot\boldsymbol{\sigma'})(\boldsymbol{\tau}\cdot\boldsymbol{\tau'}) \tag{2.2}$$

by adding a density-dependent form factor $F_{\sigma\tau}(n)$ to each term gives the CDM3Yn interaction model

$$\begin{aligned} v(n,r) = {} & F_{00}(n)v_{00}(r) + F_{10}(n)v_{10}(r)\boldsymbol{\sigma}\cdot\boldsymbol{\sigma'} \\ & + F_{01}(n)v_{01}(r)\boldsymbol{\tau}\cdot\boldsymbol{\tau'} + F_{11}(n)v_{11}(r)(\boldsymbol{\sigma}\cdot\boldsymbol{\sigma'})(\boldsymbol{\tau}\cdot\boldsymbol{\tau'}) \end{aligned} \tag{2.3}$$

where each radial term is the superposition of 3 Yukawa potentials

$$v_{\sigma\tau}(r) = \sum_{k=1}^{3} Y_{\sigma\tau}(k)\frac{\exp(-\mu_k r)}{\mu_k r} \tag{2.4}$$

and the form factor $F_{\sigma\tau}(n)$ shared the functional form (Khoa et al., 1997; Tan et al., 2020, 2021; Thân, 2010)

$$F_{\sigma\tau}(n) = C_{\sigma\tau}[1 + \alpha_{\sigma\tau}\exp(-\beta_{\sigma\tau}n) + \gamma_{\sigma\tau}n] \tag{2.5}$$

with parameters given in Table 2.1. The parameters of F_{00} were adjusted to give the corresponding incompressibility K of symmetric NM at saturation density n_0 and the binding energy $E_0 \approx 15.8\ MeV$, while the 10 term is modified from (Thân, 2010) to reproduce $E_{sym}(n_0) \approx 30\ MeV$, $L \approx 50\ MeV$ and to be in agreement with the ab-initio results (Akmal et al., 1998; Gandolfi et al., 2010) at higher density (Tan et al., 2021). On the other hand, the spin-dependent terms, 10 and 11, are hereby included in the 5 models by fine tuning the parameters to yield the same result as the Brueckner-Hartree-Fock (BHF) study of spin polarized NM (Vidana and Bombaci, 2002) as in Figure 2.1.

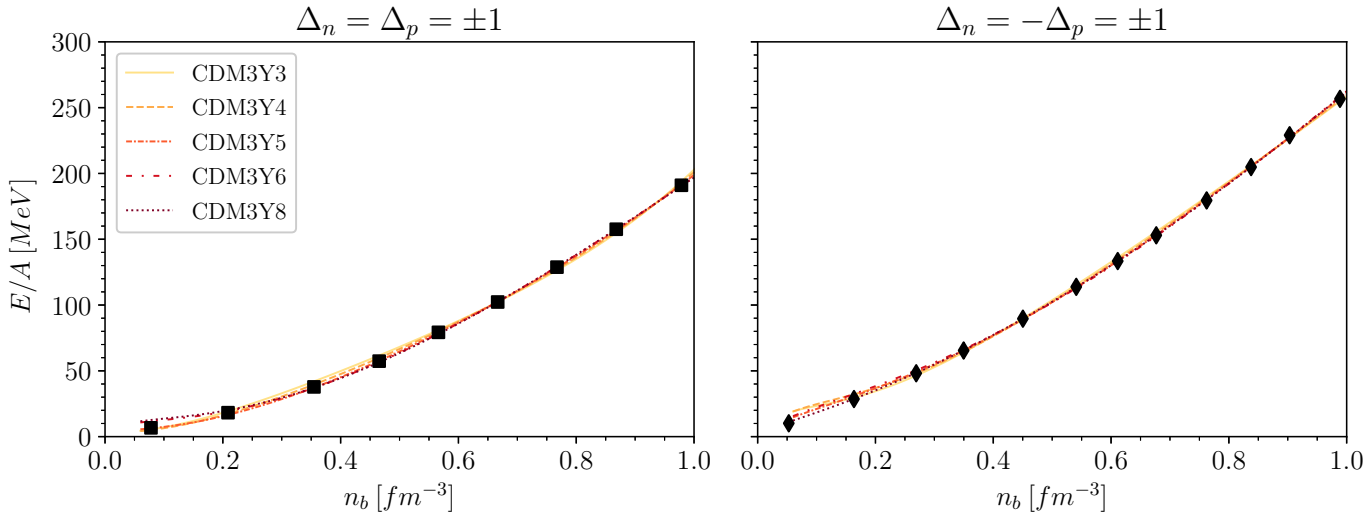

Figure 2.1: Energy per baryon E/A of symmetric NM by the 5 CDM3Yn models compared to BHF result (Vidana and Bombaci, 2002). The diamond and square represent the BHF result for $\Delta_n = -\Delta_p = \pm 1$ and $\Delta_n = \Delta_p = \pm 1$ respectively with Δ_τ being the baryon spin polarization.

2.2 Equation of States of Nuclear Matter

In HF formalism, the total HF energy of the system can be expressed as

$$E_{HF} = \sum_{\sigma\tau} \sum_{\boldsymbol{k}}^{k_F^{\sigma\tau}} \frac{\hbar^2 k^2}{2m_\tau} + \frac{1}{2} \sum_{\boldsymbol{k}\sigma\tau} \sum_{\boldsymbol{k'}\sigma'\tau'} \Big[\Big\langle \boldsymbol{k}\sigma\tau, \boldsymbol{k'}\sigma'\tau' \Big| v^D \Big| \boldsymbol{k}\sigma\tau, \boldsymbol{k'}\sigma'\tau' \Big\rangle + \Big\langle \boldsymbol{k}\sigma\tau, \boldsymbol{k'}\sigma'\tau' \Big| v^{EX} \Big| \boldsymbol{k'}\sigma\tau, \boldsymbol{k}\sigma'\tau' \Big\rangle \Big] \tag{2.6}$$

where the single-particle wave function is plane wave

$$|\boldsymbol{k}\sigma\tau\rangle = \frac{e^{i\boldsymbol{k}\cdot\boldsymbol{r}}}{\sqrt{\Omega}} \chi_\sigma \chi_\tau \tag{2.7}$$

Ω being the spatial volume of the system, $k_F^{\sigma\tau} = (6\pi^2 n_{\sigma\tau})^{1/3}$ is the Fermi momentum corresponding to spin σ and isospin τ, $v^{D(EX)}$ is the direct (exchange) part of the interaction determined from the singlet

Table 2.1: CDM3Yn interaction's parameters; the 00 and 01 terms are inherited from (Tan et al., 2021), while the 10 and 11 parameters are added by fitting with BHF result and K is the incompressibility of NM.

Interaction	$\sigma\tau$	$C_{\sigma\tau}$	$\alpha_{\sigma\tau}$	$\beta_{\sigma\tau}$ (fm^3)	$\gamma_{\sigma\tau}$ (fm^3)	K (MeV)
CDM3Y3	00	0.2985	3.4528	2.6388	−1.5	217
	01	0.2343	5.3336	6.4738	4.3172	
	10	0.3890	3.5635	−2.6717	20.3624	
	11	0.8802	4.0433	12.3262	0.3662	
CDM3Y4	00	0.3052	3.2998	2.3180	−2.0	228
	01	0.2129	6.3581	7.0584	5.6091	
	10	0.2593	6.0016	−2.3377	18.8725	
	11	0.8329	3.5941	9.2012	0.2690	
CDM3Y5	00	0.2728	3.7367	1.8294	−3.0	241
	01	0.2204	6.6146	7.9910	6.0040	
	10	0.4106	5.6265	−1.6698	−1.9866	
	11	0.6815	2.5833	5.1700	0.2578	
CDM3Y6	00	0.2658	3.8033	1.4099	−4.0	252
	01	0.2313	6.6865	8.6775	6.0182	
	10	0.5186	9.9402	1.6698	2.9799	
	11	0.6058	3.1947	4.4512	0.0822	
CDM3Y8	00	0.2658	3.8033	1.4099	−4.3	257
	01	0.2643	6.3836	9.8950	5.4249	
	10	0.5997	9.1900	0.7514	−4.7181	
	11	0.3786	3.9435	2.7012	0.3512	

and triplet-even (odd) of the central NN force. Adopting the same functional form of (2.3), the direct and exchange interaction is written as

$$\begin{aligned} v^{D(EX)}(n_b, r) = F_{00}(n_b)v_{00}^{D(EX)}(r) + F_{10}(n_b)v_{10}^{D(EX)}(r)\boldsymbol{\sigma}\cdot\boldsymbol{\sigma'} \\ + F_{01}(n_b)v_{01}^{D(EX)}(r)\boldsymbol{\tau}\cdot\boldsymbol{\tau'} + F_{11}(n_b)v_{11}^{D(EX)}(r)(\boldsymbol{\sigma}\cdot\boldsymbol{\sigma'})(\boldsymbol{\tau}\cdot\boldsymbol{\tau'}) \end{aligned} \tag{2.8}$$

and

$$v_{\sigma\tau}^{D(EX)}(r) = \sum_{k=1}^{3} Y_{\sigma\tau}^{D(EX)}(k)\frac{\exp(-\mu_k r)}{\mu_k r} \tag{2.9}$$

with the Yukawa strengths given in Table 2.2 and the density-dependent form factor parameters are in Table 2.1. Note that in (2.8), n_b denotes the *baryon density*, this will be used in order to distinguish with the lepton density in the later section.

Table 2.2: Yukawa strengths of the M3Y-Paris interaction (Tan et al., 2020; Anantaraman et al., 1983).

k	μ_k (fm^{-1})	Y_{00}^D (MeV)	Y_{10}^D (MeV)	Y_{01}^D (MeV)	Y_{11}^D (MeV)	Y_{00}^{EX} (MeV)	Y_{10}^{EX} (MeV)	Y_{01}^{EX} (MeV)	Y_{11}^{EX} (MeV)
1	4.0	11061.625	938.875	313.625	−969.125	−1524.25	−3492.75	−4118.0	−2210.0
2	2.5	−2537.5	−36.0	223.5	450.0	−518.75	795.25	1054.75	568.75
3	0.7072	0.0	0.0	0.0	3.4877	−7.8474	2.6157	2.6157	−0.8719

Multiply (2.6) with Ω^{-1}, the energy density of the NM is separated into the kinetic term ε_{kin} and the potential terms $\varepsilon_{\sigma\tau}$, i.e.

$$\varepsilon_{HF} = \frac{E_{HF}}{\Omega} = \varepsilon_{kin} + F_{00}(n_b)\varepsilon_{00} + F_{01}(n_b)\varepsilon_{01} + F_{10}(n_b)\varepsilon_{10} + F_{11}(n_b)\varepsilon_{11} \tag{2.10}$$

The final expressions of each terms of the energy density are

$$\varepsilon_{kin} = \frac{3}{10}\sum_{\sigma\tau}\frac{\hbar^2(k_F^{\sigma\tau})^2}{m_\tau}n_{\sigma\tau} \tag{2.11}$$

$$\varepsilon_{00} = \frac{1}{2}\left[n_b^2 J_{00}^D + \int A_{00}^2 v_{00}^{EX}(r)\, d^3r\right] \tag{2.12}$$

$$\varepsilon_{10} = \frac{1}{2}\left[n_b^2 J_{10}^D\left(\Delta_n\frac{1+\delta}{2} + \Delta_p\frac{1-\delta}{2}\right)^2 + \int A_{10}^2 v_{10}^{EX}(r)\, d^3r\right] \tag{2.13}$$

$$\varepsilon_{01} = \frac{1}{2}\left[n_b^2 J_{01}^D\delta^2 + \int A_{01}^2 v_{01}^{EX}(r)\, d^3r\right] \tag{2.14}$$

$$\varepsilon_{11} = \frac{1}{2}\left[n_b^2 J_{11}^D\left(\Delta_n\frac{1+\delta}{2} - \Delta_p\frac{1-\delta}{2}\right)^2 + \int A_{11}^2 v_{11}^{EX}(r)\, d^3r\right] \tag{2.15}$$

where $\Delta_\tau = (n_{\uparrow\tau} - n_{\downarrow\tau})/n_\tau$ is the polarization of nucleon, $\delta = (n_n - n_p)/n_b$ is the asymmetry of NM, $J_{\sigma\tau}^D = \int v_{\sigma\tau}^D(r)\, d^3r$ is the volume integral of the direct interaction and

$$\begin{aligned}
A_{00} &= n_{\uparrow n}\hat{j}_1(k_F^{\uparrow n}r) + n_{\downarrow n}\hat{j}_1(k_F^{\downarrow n}r) + n_{\uparrow p}\hat{j}_1(k_F^{\uparrow p}r) + n_{\downarrow p}\hat{j}_1(k_F^{\downarrow p}r)\\
A_{10} &= n_{\uparrow n}\hat{j}_1(k_F^{\uparrow n}r) - n_{\downarrow n}\hat{j}_1(k_F^{\downarrow n}r) + n_{\uparrow p}\hat{j}_1(k_F^{\uparrow p}r) - n_{\downarrow p}\hat{j}_1(k_F^{\downarrow p}r)\\
A_{01} &= n_{\uparrow n}\hat{j}_1(k_F^{\uparrow n}r) + n_{\downarrow n}\hat{j}_1(k_F^{\downarrow n}r) - n_{\uparrow p}\hat{j}_1(k_F^{\uparrow p}r) - n_{\downarrow p}\hat{j}_1(k_F^{\downarrow p}r)\\
A_{11} &= n_{\uparrow n}\hat{j}_1(k_F^{\uparrow n}r) - n_{\downarrow n}\hat{j}_1(k_F^{\downarrow n}r) - n_{\uparrow p}\hat{j}_1(k_F^{\uparrow p}r) + n_{\downarrow p}\hat{j}_1(k_F^{\downarrow p}r)
\end{aligned} \tag{2.16}$$

with $\hat{j}_1(x) = 3j_1(x)/x$ and $j_1(x)$ being the 1st order spherical Bessel function.

In the parabolic approximation (Khoa et al., 1996), the energy density per nucleon E/A can also be expanded in terms of the asymmetry δ as

$$\frac{E}{A}(n_b, \delta, \Delta_n, \Delta_p) = \frac{\varepsilon_{HF}}{n_b} = \frac{E}{A}(n_b, \delta = 0, \Delta_n, \Delta_p) + S(n_b, \Delta_n, \Delta_p)\delta^2 + \mathcal{O}(\delta^4) \tag{2.17}$$

with S being the *nuclear symmetry energy*. The symmetry coefficient J, slope parameter L and curvature K_{sym} are taken by expanding the symmetry energy at saturation density n_0, i.e. (Tan et al., 2020; Li et al., 2008; Horowitz et al., 2014; Lattimer, 2014)

$$S(n_b, \Delta_n, \Delta_p) = J(\Delta_n, \Delta_p) + \frac{L(\Delta_n, \Delta_p)}{3}\left(\frac{n_b - n_0}{n_0}\right) + \frac{K_{sym}(\Delta_n, \Delta_p)}{18}\left(\frac{n_b - n_0}{n_0}\right)^2 + \dots \tag{2.18}$$

along with the nuclear incompressibility at saturation density

$$K(\Delta_n, \Delta_p) = 9\left.\frac{\partial P(n_b, \delta = 0, \Delta_n, \Delta_p)}{\partial n_b}\right|_{n_b \to n_0} \tag{2.19}$$

These are the quantity that will be used in order to compared with the empirical values in Chapter 4.

2.3 β-Stable Nuclear Matter

After the HF calculation, we were able to obtain a numerical HF energy density $\varepsilon(n_n, n_p, \Delta_n, \Delta_p)$. However, it is in fact impossible for a NS to exist while consisting of purely nucleon. In order to compensate for this issue, leptons (e^- and μ^-) have to be introduced to the matter constituents and the $npe\mu$ matter has to satisfy the *β-stable* condition (Glendenning, 2012), i.e.

- Charge balance
$$n_p = n_e + n_\mu \tag{2.20}$$
- Chemical potential balance
$$\mu_n - \mu_p = \mu_e = \mu_\mu \tag{2.21}$$
where $\mu_i = \frac{\partial \varepsilon}{\partial n_i}$ $(i = n, p, e, \mu)$ is the chemical potential of the i particle.

The total energy density of the $npe\mu$ matter is thus

$$\varepsilon = \varepsilon_{HF} + n_n m_n c^2 + n_p m_p c^2 + \varepsilon_e + \varepsilon_\mu \tag{2.22}$$

which leads to the nucleon chemical potential of the form

$$\mu_\tau(n_n, n_p, \Delta_n, \Delta_p) = \frac{\partial \varepsilon}{\partial n_\tau} = \frac{\partial \varepsilon_{HF}}{\partial n_\tau} + m_\tau c^2 \tag{2.23}$$

Let $\hat{\mu} = \mu_n - \mu_p$ be the leptons' chemical potential, (2.20) is equivalent to[1]

$$3\pi^2(\hbar c)^3 n_p - \hat{\mu}^3 - \left[\hat{\mu}^2 - (m_\mu c^2)^2\right]^{3/2}\theta(\hat{\mu} - m_\mu c^2) = 0 \tag{2.24}$$

from which the proton fraction $x_p = n_p/n_b$ can be obtained as shown in Figure 4.1, note that only beyond the muon threshold density $\mu_e > m_\mu c^2 \approx 105.6\, MeV$ do muons appear in the system. Furthermore, under strong magnetic field like that of a magnetar, we can approximate $\Delta_n \approx -\Delta_p \approx \Delta$ and reduce

[1] $\theta(x)$ is the Heaviside function, i.e. it returns 1 for $x \geq 0$ and 0 otherwise.

the EoS to depend on just the baryon polarization Δ alone, and the more baryon polarized, the stronger the magnetic field of the NS.

For a fixed value of Δ, we are able to obtain a density function of the form $n_n(n_b, \Delta)$ and $n_p(n_b, \Delta)$, which in turn gives the lepton chemical potential $\hat{\mu}(n_b, \Delta) = \hat{\mu}(n_n, n_p)$ On the other hand, the leptons' densities are then (Loan et al., 2011)

$$n_e(n_b, \Delta) = \frac{\hat{\mu}^3(n_b, \Delta)}{3\pi^2(\hbar c)^3} \quad \text{and} \quad n_\mu(n_b, \Delta) = \frac{\left[\hat{\mu}^2(n_b, \Delta) - (m_\mu c^2)^2\right]^{3/2}}{3\pi^2(\hbar c)^3}\theta(\hat{\mu}(n_b, \Delta) - m_\mu c^2) \tag{2.25}$$

Consider the e^- and μ^- to be systems of relativistic Fermi gas, then their respective energy densities and pressure contributions are $(l = e, \mu)$ (Moustakidis and Panos, 2009)

$$\varepsilon_l(n_b, \Delta) = \frac{2}{(2\pi)^3}\int_0^{[3\pi^2 n_l(n_b,\Delta)]^{1/3}} \sqrt{\hbar^2c^2k^2 + m_l^2c^4}\, d^3\mathbf{k} \tag{2.26}$$

and

$$P_l(n_b, \Delta) = \frac{1}{3}\frac{2}{(2\pi)^3}\int_0^{[3\pi^2 n_l(n_b,\Delta)]^{1/3}} \frac{\hbar^2c^2k^2}{\sqrt{\hbar^2c^2k^2 + m_l^2c^4}}\, d^3\mathbf{k} \tag{2.27}$$

Plus, from the HF formalism with NM, the baryon pressure is given by

$$P_b = n_b^2\frac{\partial(\varepsilon_{HF}/n_b)}{\partial n_b} \tag{2.28}$$

Finally, we obtain the total energy density dependence on baryon density as

$$\varepsilon(n_b, \Delta) = \varepsilon_{HF}(n_b, \Delta) + n_n(n_b, \Delta)m_nc^2 + n_p(n_b, \Delta)m_pc^2 + \varepsilon_e(n_b, \Delta) + \varepsilon_\mu(n_b, \Delta) \tag{2.29}$$

and the total pressure of NS matter

$$P(n_b, \Delta) = P_b(n_b, \Delta) + P_e(n_b, \Delta) + P_\mu(n_b, \Delta) \tag{2.30}$$

In addition, the EoS of the NS's crust (low baryon density region) is adopted from the Compress Liquid Drop Model calculation (Douchin et al., 2000; Douchin and Haensel, 2001). The complete EoS of cold β-stable NS matter is then given in Figure 4.2 and 4.3.

Chapter 3

Neutron Star Properties

3.1 Tolman-Oppenheimer-Volkoff Equation

Suppose the NS to be static and spherically symmetric, the metric elements are then (Glendenning, 2012)

$$\mathrm{d}s^2 = g_{\mu\nu}\mathrm{d}x^\mu \mathrm{d}x^\nu = e^{2\nu(r)}c^2\mathrm{d}t^2 - e^{2\lambda(r)}\mathrm{d}r^2 - r^2\mathrm{d}\theta^2 - r^2\sin^2\theta\mathrm{d}\phi^2 \tag{3.1}$$

Consider the NS matter to be perfect fluid, the energy-momentum tensor of its has the from of

$$T^{\mu\nu} = -Pg^{\mu\nu} + (P+\varepsilon)u^\mu u^\nu \tag{3.2}$$

where $u^\mu = dx^\mu/d\tau$ is the local fluid 4-velocity. Solving the Einstein's field equation

$$G^{\mu\nu} = -\frac{8\pi G}{c^4}T^{\mu\nu} \tag{3.3}$$

gives the Tolman-Oppenheimer-Volkoff (TOV) equation (Glendenning, 2012)

$$\frac{\mathrm{d}P}{\mathrm{d}r} = -\frac{G\varepsilon(P)m}{c^2r^2}\left(1+\frac{P}{\varepsilon(P)}\right)\left(1+\frac{4\pi Pr^3}{mc^2}\right)\left(1-\frac{2Gm}{c^2r}\right)^{-1} \tag{3.4}$$

$$\frac{\mathrm{d}m}{\mathrm{d}r} = \frac{4\pi r^2\varepsilon(P)}{c^2} \tag{3.5}$$

where $\varepsilon(P)$ is the EoS obtained from the CDM3Yn interaction calculated previously. Additional boundary conditions are

$$P(0) = P_c; \qquad P(R) = 0; \qquad m(0) = 0; \qquad m(R) = M$$

and by varying the center pressure P_c, a relation of the gravitational mass M and radius R of the NS can be obtained.

3.2 Gravito-electric and Gravito-magnetic Tidal Deformation

In close orbit with another compact companion in a binary system, the NS is tidally deformed by strong gravitational interaction. Analogous to the classical theory of electromagnetism, the tidal field

experienced by it can be decomposed into 2 types: the *gravito-electric* and *gravito-magnetic* components with respective *relativistic tidal moment* (Damour and Nagar, 2009)

$$\mathcal{E}_L = \partial_{L-1} E_{a_l} \qquad \text{and} \qquad \mathcal{M}_L = c^2 \partial_{L-1} B_{a_l} \tag{3.6}$$

where E_{a_l} and B_{a_l} are the a_l component of the externally generated local GE and GM field, L represents the multi-index $(a_1, a_2, \ldots, a_l)$ and l being the order of the moment. As a result, the deformation of NS is parameterized by the GE and GM *tidal deformabilities* λ_l and σ_l, i.e. in leading order (Damour and Nagar, 2009)

$$\mathcal{Q}_L = \lambda_l \mathcal{E}_L, \tag{3.7}$$

$$\mathcal{S}_L = \sigma_l \mathcal{M}_L \tag{3.8}$$

with $\mathcal{Q}_L$ being the induced mass multipole moment, i.e. the deviation of the mass distribution from spherically symmetry at order l, while $\mathcal{S}_L$ is the current multipole moment in adiabatic approximation (Damour and Nagar, 2009; Perot and Chamel, 2021). From the deformabilities, the dimensionless GE and GM *tidal Love numbers* are defined as (Perot and Chamel, 2021)

$$k_l = \frac{1}{2}(2l-1)!! \frac{G\lambda_l}{R^{2l+1}} \quad \text{and} \quad j_l = 4(2l-1)!! \frac{G\sigma_l}{R^{2l+1}} \tag{3.9}$$

These parameters are related to the GE and GM *tidal deformability parameters* as

$$\Lambda_l = \frac{2}{(2l-1)!!} k_l \left(\frac{c^2 R}{GM}\right)^{2l+1} \tag{3.10}$$

$$\Sigma_l = \frac{1}{4(2l-1)!!} j_l \left(\frac{c^2 R}{GM}\right)^{2l+1} \tag{3.11}$$

which can be potentially extracted from the signal of GW. In order to properly calculate these parameters, let $H_l(r)$ and $\tilde{H}_l(r)$ characterize small perturbations of the static metric. These functions have to satisfy (Perot and Chamel, 2021; Damour and Nagar, 2009)

$$\begin{aligned} &H_l''(r) + H_l'(r)\left[1 - \frac{2Gm(r)}{c^2 r}\right]^{-1} \left\{\frac{2}{r} - \frac{2Gm(r)}{c^2 r^2} - \frac{4\pi G}{c^4} r[\varepsilon(r) - P(r)]\right\} \\ &+ H_l(r)\left[1 - \frac{2Gm(r)}{c^2 r}\right]^{-1} \left\{\frac{4\pi G}{c^4}\left[5\varepsilon(r) + 9P(r) + c^2 \frac{\mathrm{d}\varepsilon}{\mathrm{d}P}[\varepsilon(r) + P(r)]\right]\right. \\ &\left. - \frac{l(l+1)}{r^2} - 4\left[1 - \frac{2Gm(r)}{c^2 r}\right]^{-1} \left[\frac{Gm(r)}{c^2 r^2} + \frac{4\pi G}{c^4} r P(r)\right]^2 \right\} = 0 \end{aligned} \tag{3.12}$$

for GE perturbations and

$$\begin{aligned} &\tilde{H}_l''(r) - \tilde{H}_l'(r)\left[1 - \frac{2Gm(r)}{c^2 r}\right]^{-1} \frac{4\pi G}{c^4} r\,[P(r) + \varepsilon(r)] \\ &- \tilde{H}_l(r)\left[1 - \frac{2Gm(r)}{c^2 r}\right]^{-1} \left\{\frac{l(l+1)}{r^2} - \frac{4Gm(r)}{c^2 r^3} + \theta \frac{8\pi G}{c^4}[P(r) + \varepsilon(r)]\right\} = 0 \end{aligned} \tag{3.13}$$

for GM perturbations; the value of $\theta = 1$ is for static fluid while irrotational fluid adopts the value $\theta = -1$. These two equations are integrated along with the TOV equation (3.4). In addition, we have the compactness parameters $C = GM/(Rc^2)$ and define

$$y_l = \frac{RH_l'(R)}{H_l(R)} \quad \text{and} \quad \tilde{y}_l = \frac{R\tilde{H}_l'(R)}{\tilde{H}_l(R)}. \tag{3.14}$$

The explicit expressions of the first few orders of the GE and GM Love numbers are (Perot and Chamel, 2021)

$$\begin{aligned}
k_2 &= \frac{8}{5}C^5(1-2C)^2\left[2(y_2-1)C-y_2+2\right]\Big\{2C\Big[4(y_2+1)C^4+2(3y_2-2)C^3 \\
&\quad -2(11y_2-13)C^2+3(5y_2-8)C-3(y_2-2)\Big] \\
&\quad +3(1-2C)^2\left[2(y_2-1)C-y_2+2\right]\log(1-2C)\Big\}^{-1}, \qquad (3.15)\\
k_3 &= \frac{8}{7}C^7(1-2C)^2\Big[2(y_3-1)C^2-3(y_3-2)C+y_3-3\Big] \\
&\quad \times\Big\{2C\Big[4(y_3+1)C^5+2(9y_3-2)C^4-20(7y_3-9)C^3+5(37y_3-72)C^2-45(2y_3-5)C \\
&\quad +15(y_3-3)\Big]+15(1-2C)^2\Big[2(y_3-1)C^2-3(y_3-2)C+y_3-3\Big]\log(1-2C)\Big\}^{-1}, \qquad (3.16)\\
k_4 &= \frac{32}{147}C^9(1-2C)^2\Big[12(y_4-1)C^3-34(y_4-2)C^2+28(y_4-3)C-7(y_4-4)\Big] \\
&\quad \times\Big\{2C\Big[8(y_4+1)C^6+4(17y_4-2)C^5-12(83y_4-107)C^4+40(55y_4-116)C^3 \\
&\quad -10(191y_4-536)C^2+105(7y_4-24)C-105(y_4-4)\Big]+15(1-2C)^2\Big[12(y_4-1)C^3 \\
&\quad -34(y_4-2)C^2+28(y_4-3)C-7(y_4-4)\Big]\log(1-2C)\Big\}^{-1}, \qquad (3.17)\\
j_2 &= \frac{24}{5}C^5\left[2(\tilde{y}_2-2)C-\tilde{y}_2+3\right]\Big\{2C\Big[2(\tilde{y}_2+1)C^3+2\tilde{y}_2C^2+3(\tilde{y}_2-1)C-3(\tilde{y}_2-3)\Big] \\
&\quad +3\left[2(\tilde{y}_2-2)C-\tilde{y}_2+3\right]\log(1-2C)\Big\}^{-1}, \qquad (3.18)\\
j_3 &= \frac{64}{21}C^7\Big[8(\tilde{y}_3-2)C^2-10(\tilde{y}_3-3)C+3(\tilde{y}_3-4)\Big] \\
&\quad \times\Big\{2C\Big[4(\tilde{y}_3+1)C^4+10\tilde{y}_3C^3+30(\tilde{y}_3-1)C^2-15(7\tilde{y}_3-18)C+45(\tilde{y}_3-4)\Big] \\
&\quad +15\Big[8(\tilde{y}_3-2)C^2-10(\tilde{y}_3-3)C+3(\tilde{y}_3-4)\Big]\log(1-2C)\Big\}^{-1}, \qquad (3.19)\\
j_4 &= \frac{80}{147}C^9\Big[40(\tilde{y}_4-2)C^3-90(\tilde{y}_4-3)C^2+63(\tilde{y}_4-4)C-14(\tilde{y}_4-5)\Big] \\
&\quad \times\Big\{2C\Big[4(\tilde{y}_4+1)C^5+18\tilde{y}_4C^4+90(\tilde{y}_4-1)C^3-5(137\tilde{y}_4-334)C^2 \\
&\quad +105(7\tilde{y}_4-26)C-210(\tilde{y}_4-5)\Big]+15\Big[40(\tilde{y}_4-2)C^3-90(\tilde{y}_4-3)C^2 \\
&\quad +63(\tilde{y}_4-4)C-14(\tilde{y}_4-5)\Big]\log(1-2C)\Big\}^{-1}
\end{aligned}$$

Chapter 4

Results and Discussions

Under the condition of β-stable, the proton's contribution $x_p = n_p/n_b$ to the baryon density of of neutrino-free NS matter is given by Figure 4.1, computed with 5 different versions of the density-dependent NN interaction. For simplicity, the baryon spin polarization Δ is assumed to be density-independent, such that it can be varied separatedly from $\Delta = 0$ (spin saturated scenario) to $\Delta = 1$ (total polarization). It can be seen from Figure 4.1 that in all cases, the higher the density, the more protons there are in the baryon composition. Furthermore, with the newly introduced parameterization of spin-dependent terms (10 and 11) in all 5 interactions, generally the protons are more abundant at higher polarization, the central density corresponding to the highest possible NS in each interaction also tends to decrease to a comparable level for each model with such change in Δ. The density-dependent

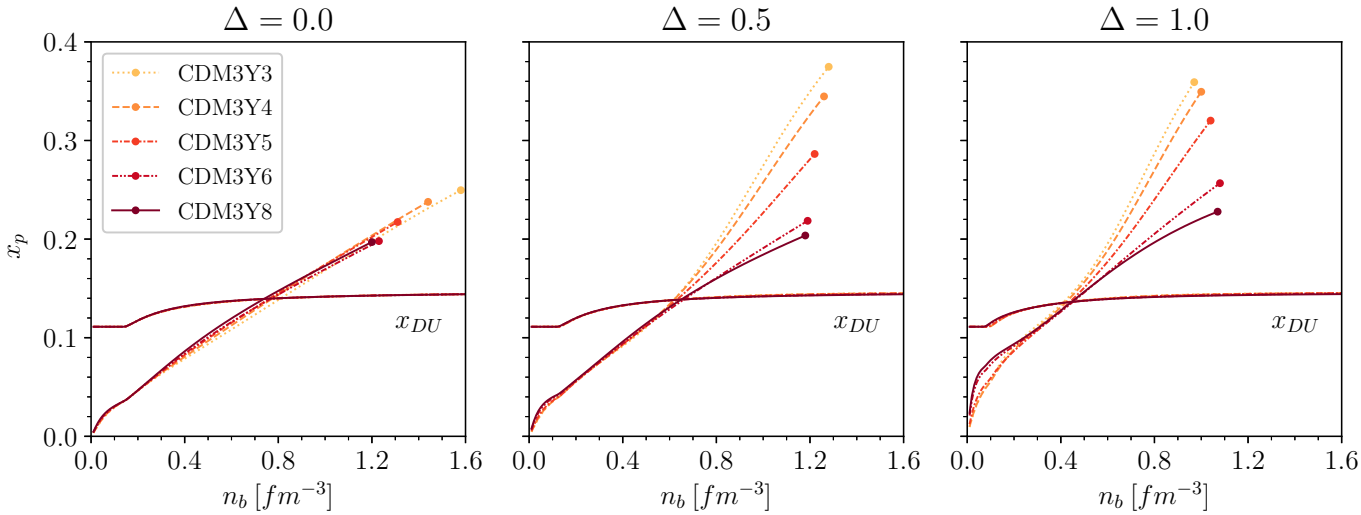

Figure 4.1: Proton fraction x_p of β-stable NM at different baryon density and spin polarization for CDM3Yn interactions. The lower horizontal lines are the DU threshold (4.2) and the dot at the end of each line corresponds to the highest mass NS's central density of each model.

proton fraction x_p is also an essential input for determining the cooling rate of the NS, in which the

dominant direct Urca (DU) process of NS cooling by ν emission (Lattimer and Prakash, 2004), i.e.

$$n \longrightarrow p + e^- + \bar{\nu}_e \quad \text{and} \quad p \longrightarrow n + e^+ + \nu_e, \tag{4.1}$$

can only take place if the proton fraction exceeds the threshold (Loan et al., 2011)

$$x_{DU} = \frac{1}{1 + \left[1 + \left(\frac{n_e}{n_e + n_\mu}\right)^{1/3}\right]^3} \tag{4.2}$$

Note that the thresholds x_{DU} determined in these calculations remain fairly unchanged in the whole range of baryon density, as well as when the polarization varies or at different models, which can be explained by the absence of interaction between leptons and baryons in the current study. The proton fraction x_p in this case increases significantly as the value of Δ rises from $0 \to 1$ and surpasses the DU threshold at much lower density of $\gtrsim 3n_0$. Beside, the electron fraction infered by this result might also reach up to $\gtrsim 20\%$ at Δ approaching 1, which is fairly compatible with the observed quantity 27% from the blue kilonova ejecta following the GW170817 event (Abbott et al., 2017; Evans et al., 2017) and can very possibly come from a magnetar as suggested by Metzger et al. (2018).

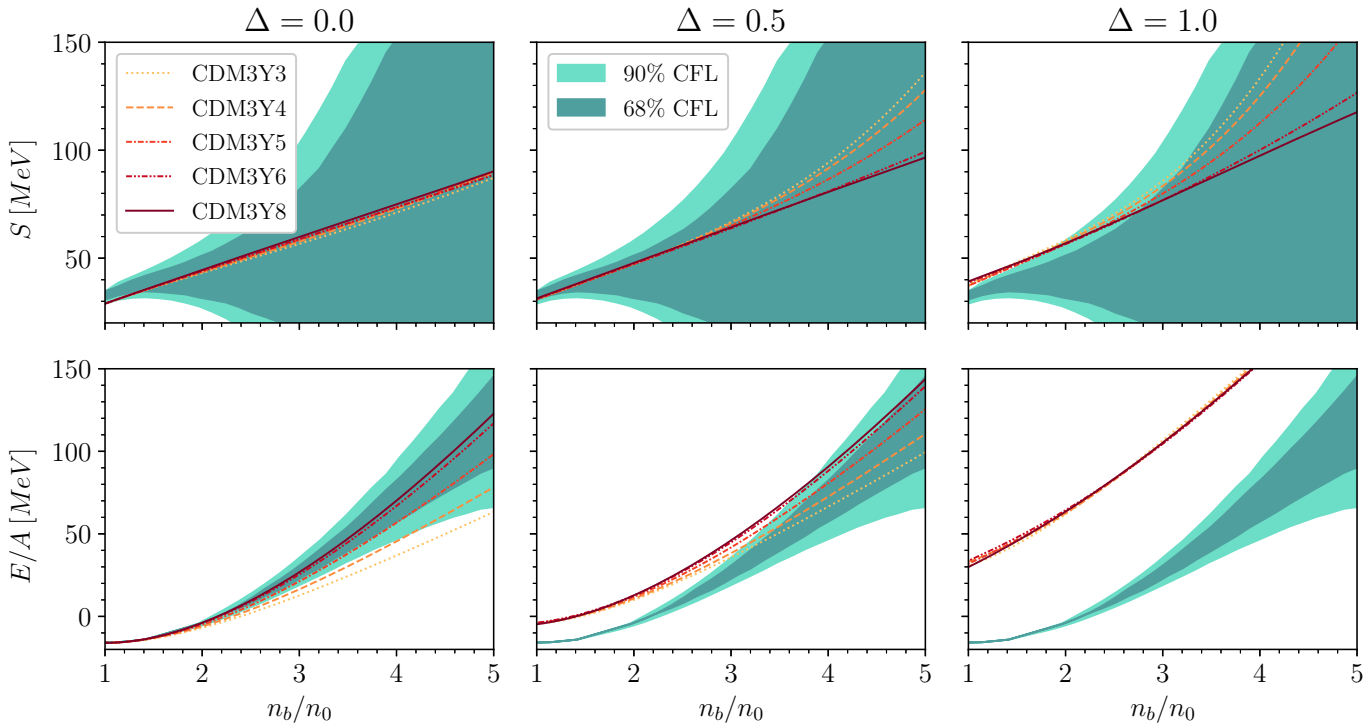

Figure 4.2: Symmetric energy S and energy per nucleon of symmetric NM at increasing polarization with 5 CDM3Yn interaction models. The shaded areas are the empirical ranges obtained from the Bayesian study (Xie and Li, 2019) of the NS of radius $R_{1.4}$ at 68% and 90% confident level (CFL) with the GW170817 event (Abbott et al., 2018).

On one hand, as shown in Figure 4.2, the total energy density of the $npe\mu$ matter doesn't vary much from each others and from different configurations, while on the other hand,

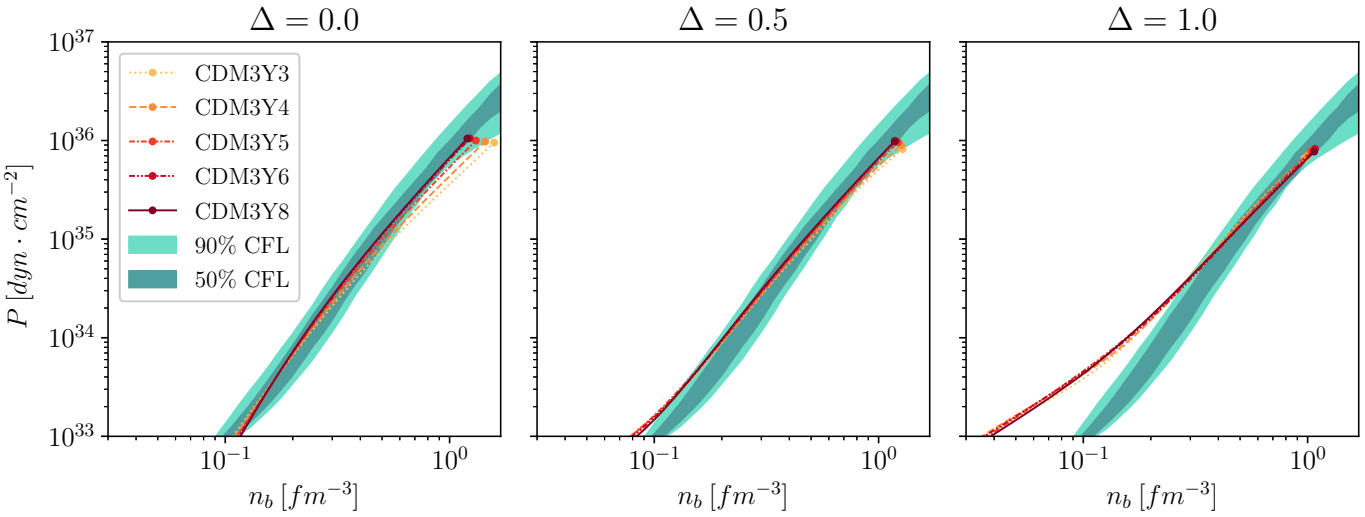

Figure 4.3: Same as Figure 4.2 for the pressure P along with empirical pressure given by the "Spectral" EoS from the Bayesian analysis of the GW170817 data (Abbott et al., 2018) with 50% (light gray) and 90% (dark gray) confidence level. The dot at the end of each line corresponds to the central baryon density n_b of maximum NS mass.

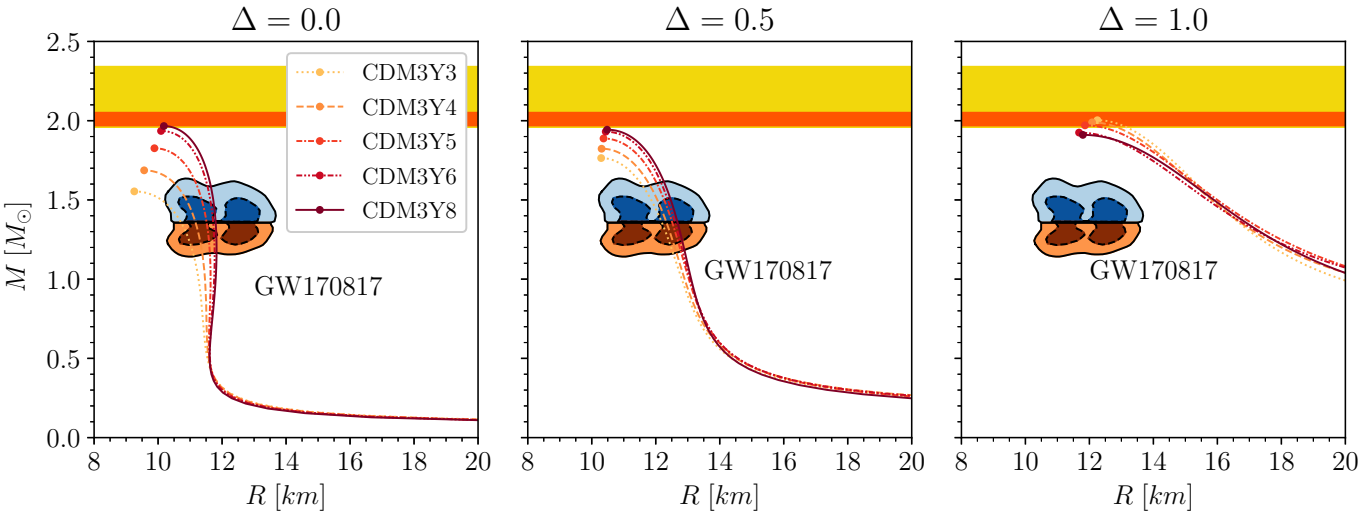

Figure 4.4: The relation between gravitational mass M and the radius R of the NS according to the corresponding model and polarization. The GW170817 constraint for NS with mass $1.4M_{\odot}$ is shown by the colored contour, where the blue (red) shaded area represents the heavier (lighter) NS (Abbott et al., 2018). The dot in each line indicates the maximum NS mass of the each model. The dark and light orange region indicates the mass of the second PSR J0348+0432 (Antoniadis et al., 2013) and millisecond PSR J0740+6620 (Cromartie et al., 2020) respectively, which are the heaviest NSs ever observed.

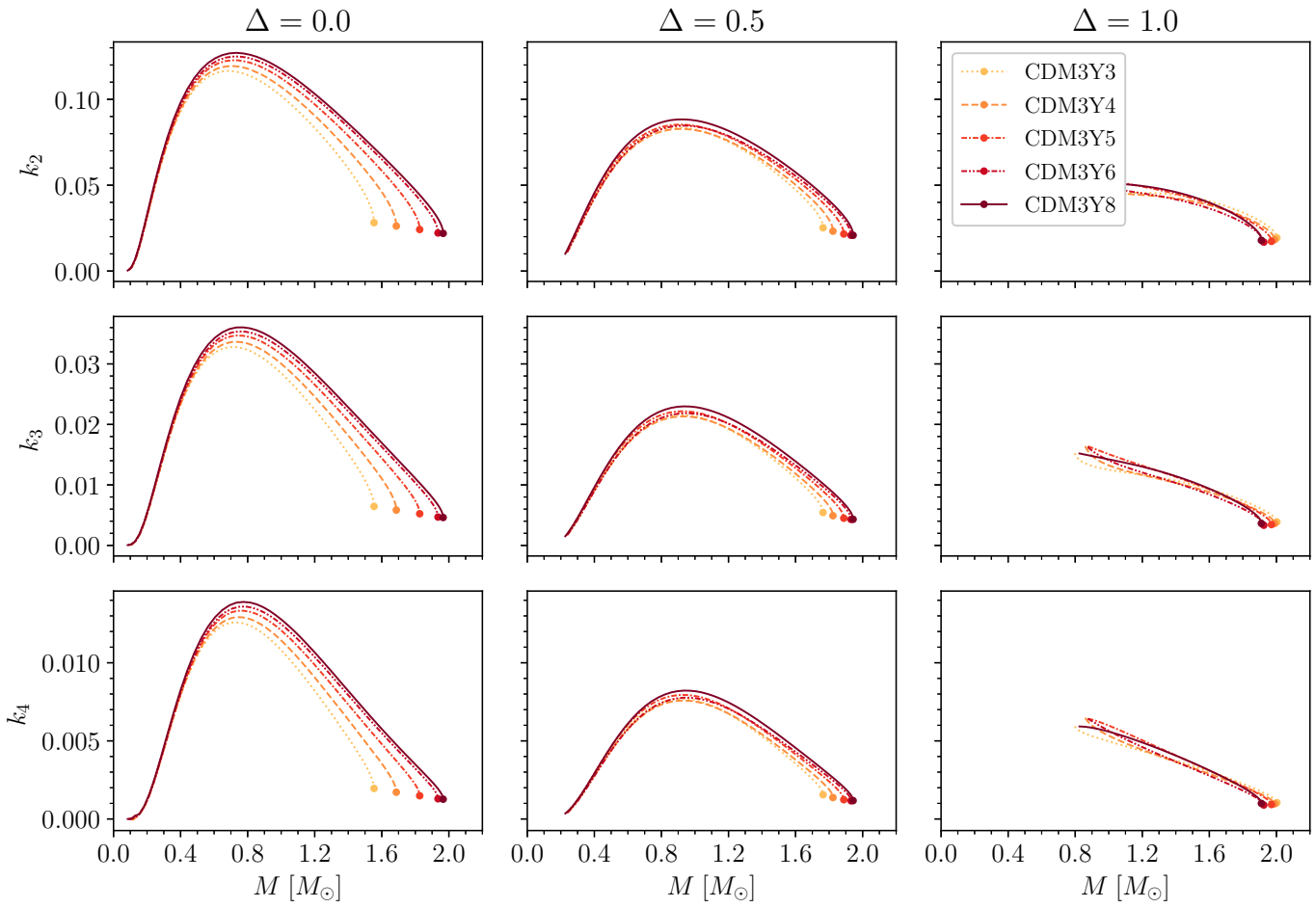

Figure 4.5: GE tidal Love number at l^{th} order k_l as function of NS mass computed with CDM3Yn models at different spin polarizations.

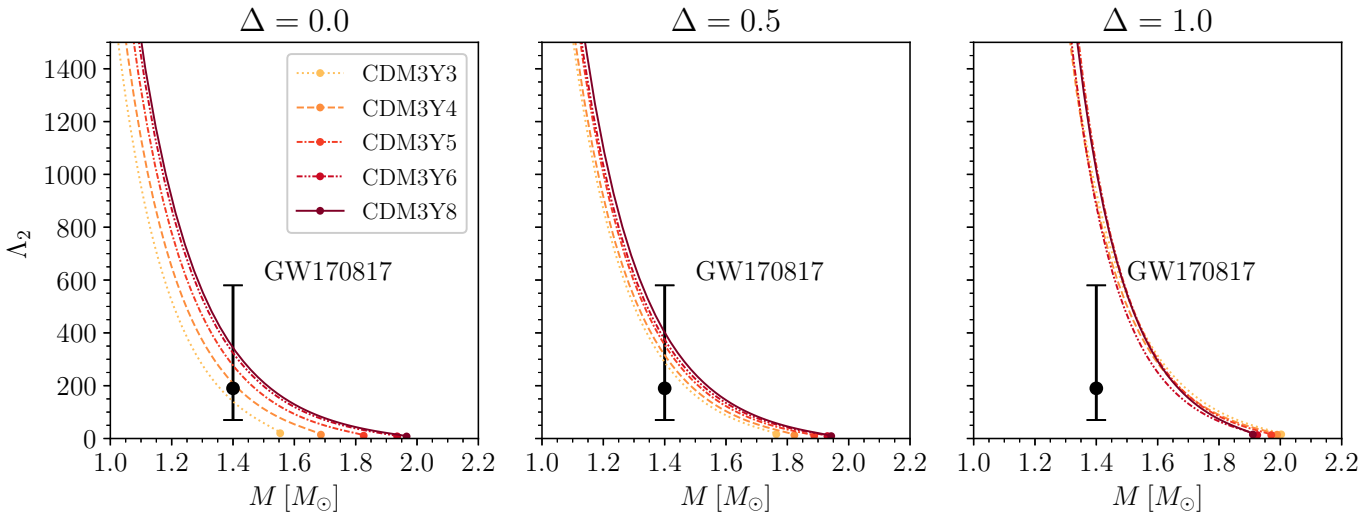

Figure 4.6: Dimensionless GE tidal deformability parameter of 2$^{\text{nd}}$ order Λ_2 of different CDM3Yn models with varying Δ. The vertical bar is the empirical tidal deformability constraint $\Lambda_2 \approx 190^{+390}_{-120}$ at $1.4M_\odot$, obtained from the Bayesian analysis of GW170817 data with 90% confidence level (Abbott et al., 2018).

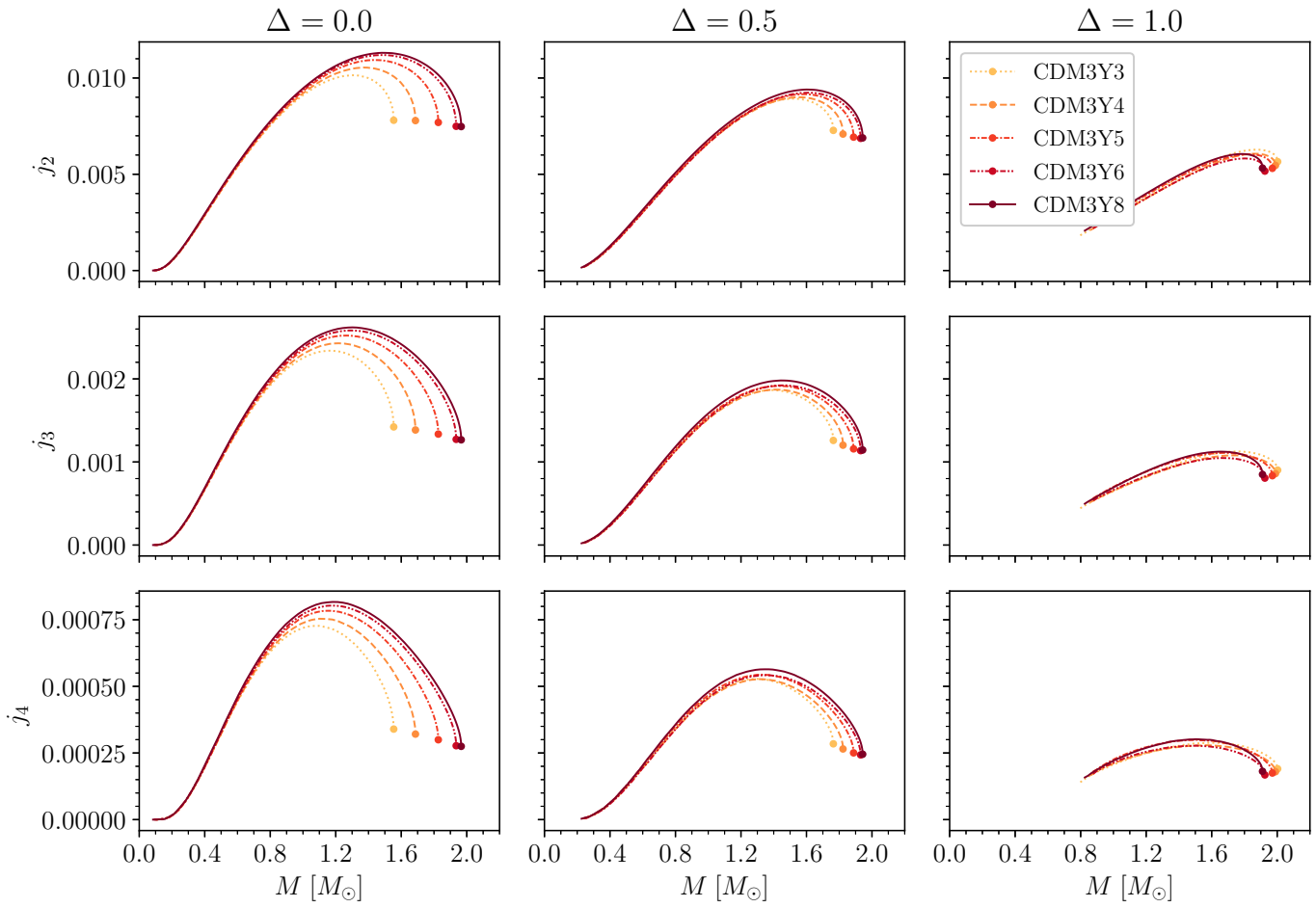

Figure 4.7: GM tidal Love number at l^{nd} order j_l as function of NS mass computed with CDM3Yn models of *strictly static fluid* at different polarizations.

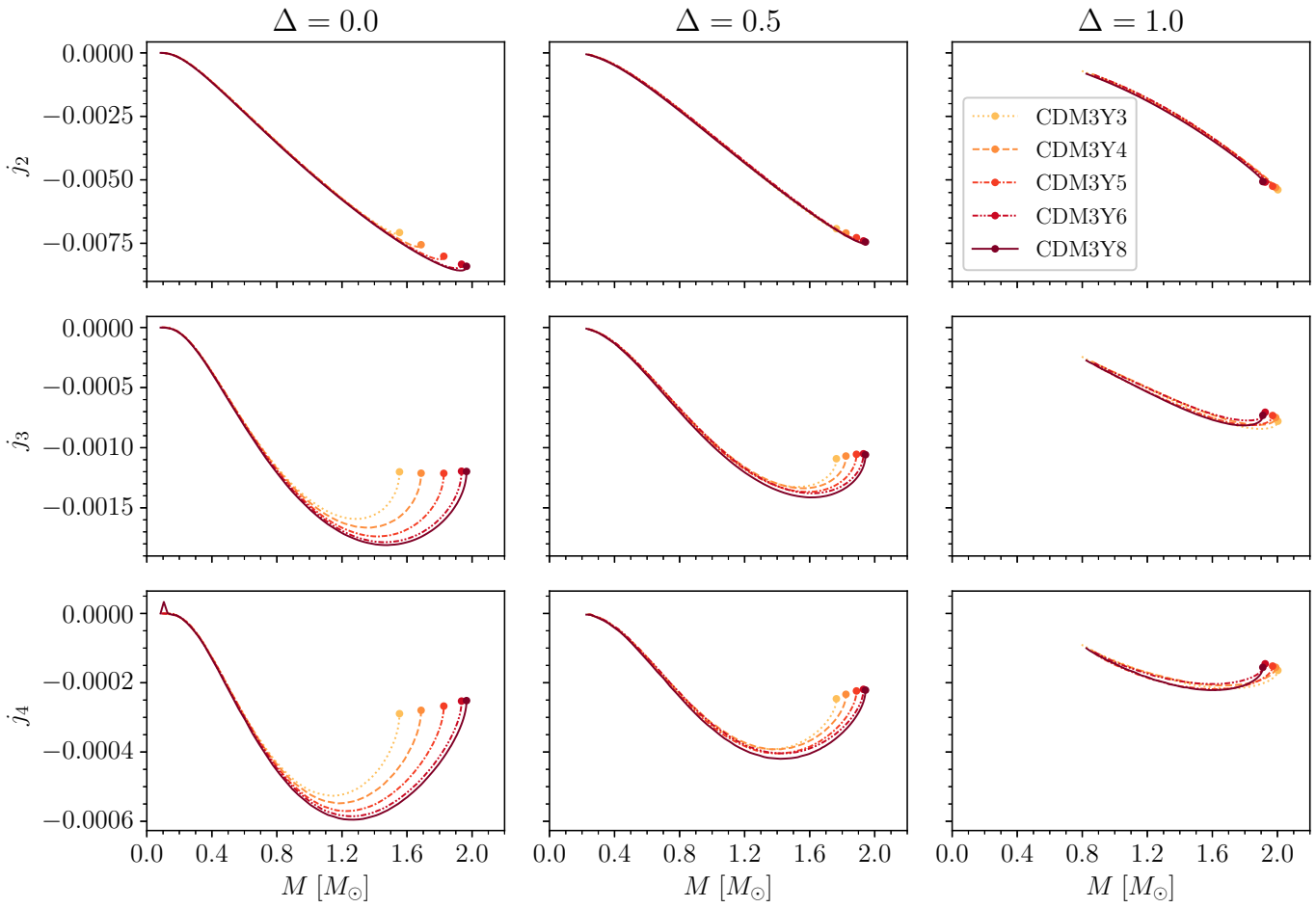

Figure 4.8: GM tidal Love number at l^{nd} order j_l as function of NS mass computed with CDM3Yn models of *irrotational fluid* at different polarizations.

Chapter 5

Conclusions

Bibliography

Abbott, B., Abbott, R., Abbott, T., Abraham, S., Acernese, F., Ackley, K., Adams, C., Adhikari, R., Adya, V., Affeldt, C., et al. (2020). GW190425: observation of a compact binary coalescence with total mass $\sim 3.4 M_{\odot}$. *The Astrophysical Journal Letters*, 892(1):L3.

Abbott, B. P., Abbott, R., Abbott, T., Acernese, F., Ackley, K., Adams, C., Adams, T., Addesso, P., Adhikari, R., Adya, V., et al. (2017). GW170817: observation of gravitational waves from a binary neutron star inspiral. *Physical Review Letters*, 119(16):161101.

Abbott, B. P., Abbott, R., Abbott, T., Acernese, F., Ackley, K., Adams, C., Adams, T., Addesso, P., Adhikari, R. X., Adya, V. B., et al. (2018). GW170817: Measurements of neutron star radii and equation of state. *Physical review letters*, 121(16):161101.

Akmal, A., Pandharipande, V., and Ravenhall, D. a. (1998). Equation of state of nucleon matter and neutron star structure. *Physical Review C*, 58(3):1804.

Anantaraman, N., Toki, H., and Bertsch, G. (1983). An effective interaction for inelastic scattering derived from the Paris potential. *Nuclear Physics A*, 398(2):269–278.

Antoniadis, J., Freire, P. C., Wex, N., Tauris, T. M., Lynch, R. S., van Kerkwijk, M. H., Kramer, M., Bassa, C., Dhillon, V. S., Driebe, T., et al. (2013). A massive pulsar in a compact relativistic binary. *Science*, 340(6131).

Baym, G. and Pethick, C. (1975). Neutron stars. *Annual Review of Nuclear Science*, 25(1):27–77.

Cromartie, H. T., Fonseca, E., Ransom, S. M., Demorest, P. B., Arzoumanian, Z., Blumer, H., Brook, P. R., DeCesar, M. E., Dolch, T., Ellis, J. A., et al. (2020). Relativistic Shapiro delay measurements of an extremely massive millisecond pulsar. *Nature Astronomy*, 4(1):72–76.

Damour, T. and Nagar, A. (2009). Relativistic tidal properties of neutron stars. *Physical Review D*, 80(8):084035.

Douchin, F. and Haensel, P. (2001). A unified equation of state of dense matter and neutron star structure. *Astronomy & Astrophysics*, 380(1):151–167.

Douchin, F., Haensel, P., and Meyer, J. (2000). Nuclear surface and curvature properties for SLy Skyrme forces and nuclei in the inner neutron-star crust. *Nuclear Physics A*, 665(3-4):419–446.

Evans, P., Cenko, S., Kennea, J., Emery, S., Kuin, N., Korobkin, O., Wollaeger, R., Fryer, C., Madsen, K., Harrison, F., et al. (2017). Swift and NuSTAR observations of GW170817: detection of a blue kilonova. *Science*, 358(6370):1565–1570.

Gandolfi, S., Illarionov, A. Y., Fantoni, S., Miller, J., Pederiva, F., and Schmidt, K. (2010). Microscopic calculation of the equation of state of nuclear matter and neutron star structure. *Monthly Notices of the Royal Astronomical Society: Letters*, 404(1):L35–L39.

Glendenning, N. K. (2012). *Compact stars: Nuclear physics, particle physics and general relativity*. Springer Science & Business Media.

Greiner, W. and Maruhn, J. A. (1996). *Nuclear models*. Springer.

Hinderer, T. (2008). Tidal Love numbers of neutron stars. *The Astrophysical Journal*, 677(2):1216.

Hinderer, T., Lackey, B. D., Lang, R. N., and Read, J. S. (2010). Tidal deformability of neutron stars with realistic equations of state and their gravitational wave signatures in binary inspiral. *Physical Review D*, 81(12):123016.

Horowitz, C., Brown, E., Kim, Y., Lynch, W., Michaels, R., Ono, A., Piekarewicz, J., Tsang, M., and Wolter, H. (2014). A way forward in the study of the symmetry energy: experiment, theory, and observation. *Journal of Physics G: Nuclear and Particle Physics*, 41(9):093001.

Khoa, D. T. and Cuong, D. C. (2007). Mean-field description of the nucleus-nucleus optical potential. *arXiv preprint arXiv:0708.3711*.

Khoa, D. T. and Satchler, G. (2000). Generalized folding model for elastic and inelastic nucleus–nucleus scattering using realistic density dependent nucleon–nucleon interaction. *Nuclear Physics A*, 668(1-4):3–41.

Khoa, D. T., Satchler, G., and Von Oertzen, W. (1997). Nuclear incompressibility and density dependent NN interactions in the folding model for nucleus-nucleus potentials. *Physical Review C*, 56(2):954.

Khoa, D. T., Von Oertzen, W., Bohlen, H., Bartnitzky, G., Clement, H., Sugiyama, Y., Gebauer, B., Ostrowski, A., Wilpert, T., Wilpert, M., et al. (1995). Equation of State for Cold Nuclear Matter from Refractive O 16+ O 16 Elastic Scattering. *Physical review letters*, 74(1):34.

Khoa, D. T., Von Oertzen, W., and Ogloblin, A. (1996). Study of the equation of state for asymmetric nuclear matter and interaction potential between neutron-rich nuclei using the density-dependent M3Y interaction. *Nuclear Physics A*, 602(1):98–132.

Lattimer, J. M. (2014). Symmetry energy in nuclei and neutron stars. *Nuclear Physics A*, 928:276–295.

Lattimer, J. M. and Prakash, M. (2004). The physics of neutron stars. *science*, 304(5670):536–542.

Le Tiec, A. and Casals, M. (2021). Spinning black holes fall in love. *Physical Review Letters*, 126(13):131102.

Li, B.-A., Chen, L.-W., and Ko, C. M. (2008). Recent progress and new challenges in isospin physics with heavy-ion reactions. *Physics Reports*, 464(4-6):113–281.

Loan, D. T., Tan, N. H., Khoa, D. T., and Margueron, J. (2011). Equation of state of neutron star matter, and the nuclear symmetry energy. *Physical Review C*, 83(6):065809.

Metzger, B. D., Thompson, T. A., and Quataert, E. (2018). A magnetar origin for the kilonova ejecta in GW170817. *The Astrophysical Journal*, 856(2):101.

Moustakidis, C. C. and Panos, C. (2009). Equation of state for β-stable hot nuclear matter. *Physical Review C*, 79(4):045806.

Perot, L. and Chamel, N. (2021). Role of dense matter in tidal deformations of inspiralling neutron stars and in gravitational waveforms with unified equations of state. *Physical Review C*, 103(2):025801.

Tan, N. H., Khoa, D. T., and Loan, D. T. (2020). Spin-polarized β-stable neutron star matter: The nuclear symmetry energy and GW170817 constraint. *Physical Review C*, 102(4):045809.

Tan, N. H., Khoa, D. T., and Loan, D. T. (2021). Equation of state of asymmetric nuclear matter and the tidal deformability of neutron star. *arXiv preprint arXiv:2104.09121*.

Tan, N. H., Loan, D. T., Khoa, D. T., and Margueron, J. (2016). Mean-field study of hot β-stable protoneutron star matter: Impact of the symmetry energy and nucleon effective mass. *Physical Review C*, 93(3):035806.

Thân, H. S. (2010). *UFR SCIENTIFIQUE D'ORSAY INSTITUT DE PHYSIQUE NUCLEAIRE D'ORSAY*. PhD thesis, Citeseer.

Vidana, I. and Bombaci, I. (2002). Equation of state and magnetic susceptibility of spin polarized isospin asymmetric nuclear matter. *Physical Review C*, 66(4):045801.

Xie, W.-J. and Li, B.-A. (2019). Bayesian inference of high-density nuclear symmetry energy from radii of canonical neutron stars. *The Astrophysical Journal*, 883(2):174.